European Journal of Medicinal Chemistry 115 (2016) 63–74

Contents lists available at ScienceDirect

European Journal of Medicinal Chemistry

journal homepage: http://www.elsevier.com/locate/ejmech

Research paper

# Applying the designed multiple ligands approach to inhibit dihydrofolate reductase and thioredoxin reductase for anti-proliferative activity

Hui-Li Ng, Shangying Chen, Eng-Hui Chew, Wai-Keung Chui*

*Department of Pharmacy, Faculty of Science, 18 Science Drive 4, National University of Singapore, 117543, Singapore*

ARTICLE INFO

*Article history:*
Received 22 November 2015
Received in revised form
29 February 2016
Accepted 2 March 2016
Available online 3 March 2016

*Keywords:*
Dihydrofolate reductase
Thioredoxin reductase
Dihydrotriazines
Chalcones
Antiproliferative activity

ABSTRACT

The development of multi-targeting drugs is currently being explored as an attractive alternative to combination therapy, especially for the treatment of complex diseases such as cancer. Dihydrofolate reductase (DHFR) and thioredoxin reductase (TrxR) are enzymes belonging to two unrelated cellular pathways that are known to contribute towards cancer cell growth and survival. In order to evaluate whether simultaneous inhibition of DHFR and TrxR by dihydrotriazines (DHFR-targeting) and chalcones (TrxR-targeting) may be beneficial, breast MCF-7 and colorectal HCT116 carcinoma cells were treated with combinations of selected dihydrotriazines and chalcones at a 1:1 M ratio. Two combinations demonstrated synergy at low-to-moderate concentrations. Based on this result, four merged dihydrotriazine-chalcone compounds were designed and synthesized. Two compounds, **11a** [DHFR $IC_{50}$ = 56.4 μM, TrxR $IC_{50}$ (60 min) = 12.6 μM] and **11b** [DHFR $IC_{50}$ = 2.4 μM, TrxR $IC_{50}$ (60 min) = 10.1 μM], demonstrated *in vitro* inhibition of DHFR and TrxR. The compounds showed growth inhibitory activity against MCF-7 and HCT116 cells, but lacked cytotoxicity. Molecular docking experiments showed **11b** to possess rational binding modes to both the enzymes. In conclusion, this study has not only identified the dihydrotriazine and chalcone scaffolds as good starting points for the development of dual inhibitors of DHFR and TrxR, but also demonstrated the synthetic feasibility of producing a chemical entity that could result in simultaneous inhibition of DHFR and TrxR. Future efforts to improve the antiproliferative profiles of such compounds will look at alternative ways of integrating the two pharmacophoric scaffolds.



## 1. Introduction

The rational design of producing a single chemical entity that is able to act on multiple targets relevant to a disease is an approach currently gaining popularity. In 2005, the term “designed multiple ligands” was coined by Morphy and Rankovic to describe such compounds [1]. In the field of cancer chemotherapy, designed multiple ligands offer several potential advantages over single target compounds. Multiple pathways of cell survival could be targeted simultaneously, leading to increased therapeutic efficacy [2] and decreased development of cancer drug resistance [3]. Additionally, the use of a single multi-targeted agent instead of administering multiple agents could help to circumvent the gruelling issues associated with complex pharmacokinetic and pharmacodynamic (PK/PD) relationships and potential drug–drug interactions [1].

Dihydrofolate reductase (DHFR) and thioredoxin reductase (TrxR) are two enzymes that are implicated in the growth and survival of cancer cells. As part of the folate pathway, DHFR catalyzes the reduction of dihydrofolic acid to tetrahydrofolic acid, which is essential for the biosynthesis of nucleic acids and amino acids. Methotrexate (MTX) is a DHFR inhibitor that has been used in the clinic as an anticancer agent for more than 60 years. However, its use has become limited by the emergence of acquired resistance to MTX by cancer cells, and this has inspired efforts to develop non-classical DHFR inhibitors that do not contain the glutamate residue found in MTX [4–6]. Being lipophilic, non-classical inhibitors enter cells via passive diffusion, thus circumventing drug resistance due to transport resistance attributed to decreased levels of or mutations in the reduced folate carrier, a putative carrier for active MTX

* Corresponding author.
*E-mail address:* phacwk@nus.edu.sg (W.-K. Chui).

http://dx.doi.org/10.1016/j.ejmech.2016.03.002
0223-5234/

transport. Additionally, since non-classical DHFR inhibitors are not polyglutamated, they are not affected by impaired polyglutamylation resulting from reduced folylpolyglutamate synthetase (FPGS) activity. Examples of non-classical DHFR inhibitors are the 4,6-diamino-1,2-dihydro-1,3,5-triazines, first synthesized by E.J. Modest in 1951 [7]. Our laboratory has interest in the design and development of this class of triazine-based compounds as non-classical DHFR inhibitors [8–10].

TrxR and its substrate thioredoxin (Trx) make up the Trx system, which plays an important role in maintaining redox homeostasis and protecting cells against oxidative damage and mutation [11,12]. However, in malignancies, the biological activities of the Trx/TrxR system contribute to tumor growth and progression. Indeed, it has been demonstrated in several human cancers that overexpression of Trx and TrxR are associated with drug resistance and poor patient prognosis [13–16]. The mammalian TrxR enzyme has a highly accessible C-terminal active site containing a penultimate selenocysteine (Sec) residue which is easily attacked by agents that possess an electrophilic center [17–19]. Among such compounds that possess electrophilic character, chalcones containing an α,β-unsaturated carbonyl moiety, also known as a Michael acceptor moiety, have recently been demonstrated to exert anti-proliferative effects against human cancer cells through selective and irreversible inhibition of TrxR [20,21]. The electrophilic β carbon atom within the α,β-unsaturated carbonyl moiety of chalcones is proposed to react irreversibly with the C-terminal Sec residue of the TrxR enzyme via a Michael addition reaction, thereby forming covalent adducts [20].

In the current study, the goal was to harness the combined benefits of simultaneous inhibition of DHFR and TrxR using compounds possessing the respective pharmacophoric scaffolds to bring about enhanced anti-cancer effect. To do this, two approaches were employed and examined. In the first approach, it was hypothesized that the combined use of a 4,6-diamino-1,2-dihydro-1,3,5-triazine and a chalcone would result in enhanced antiproliferative profiles against cancer cells in comparison to the anti-tumor activities of the individual compounds. As such, MCF-7 breast and HCT116 colorectal carcinoma cells were treated with a combination of 4,6-diamino-1,2-dihydro-1,3,5-triazines and chalcones at a 1:1 M ratio. In the second approach, it was hypothesized that the structural combination of the 4,6-diamino-1,2-dihydro-1,3,5-triazine and chalcone scaffolds would produce new molecules that possessed potent antiproliferative profiles correlated to strong DHFR and TrxR inhibitory activities. To test this hypothesis, the 4-6-diamino-1,2-dihydro-1,3,5-triazine and chalcone scaffolds were incorporated synthetically into a single chemical entity; in a preliminary attempt, four merged dihydrotriazine-chalcone compounds were synthesized and evaluated for anti-proliferative activities and possible *in vitro* inhibitory effects on DHFR and TrxR. In summary, findings obtained in this proof-of-concept study have highlighted the feasibility of producing a single chemical entity to bring about simultaneous inhibition of DHFR and TrxR, albeit the chemical approach to merge dihydrotriazine and chalcone pharmacophores to obtain dual-targeted compounds possessing well-correlated enzyme (DHFR and TrxR) inhibitory and anti-proliferative activities would need further optimization.

## 2. Results and discussion

### 2.1. Combination treatment

Two 4,6-diamino-1,2-dihydro-1,3,5-triazines, **T1** and **T2**, and three chalcones, **C1**–**C3**, were selected for this study. The structures of the compounds are shown in Fig. 1, and the enzyme inhibitory activities and antiproliferative activities of **T1**-**T2** and **C1**–**C3** are summarized in Tables 1 and 2 respectively. *In vitro* efficacy of enzyme inhibitory activity was expressed as $IC_{50}$ (50% DHFR/TrxR inhibition concentration), while antiproliferative activity was expressed as $GI_{50}$, which is the concentration of drug at which 50% of growth inhibition was achieved, and $LC_{50}$, which is the concentration of drug at which 50% of the cells were killed. As shown in Table 1, **T1** and **T2** were moderately potent inhibitors of recombinant human DHFR with $IC_{50}$ values in the low μM range. **T1** and **T2** also inhibited growth of MCF-7 and HCT116 carcinoma cells with $GI_{50}$ values in the low μM range, but were not cytotoxic as evident in the $LC_{50}$ values that were determined to be above 100 μM. This could be related to their DHFR inhibitory activities that caused cells to be unable to produce new DNA, RNA and proteins, thus resulting in growth inhibition but not necessarily cell death. As shown in Table 2, **C1**–**C3** demonstrated moderately potent inhibition of rat liver TrxR upon incubation with the enzyme for 60 min, recording $IC_{50}$ values in the μM range. As evident from the obtained $GI_{50}$ and $LC_{50}$ values in the μM range, the chalcones displayed moderately good anti-proliferative activity and exerted cytotoxicity against MCF-7 and HCT116 cell lines.

In order to evaluate whether the use of 4,6-diamino-1,2-dihydro-1,3,5-triazines and chalcones in combination would result in enhanced anti-proliferative activity, the 3-(4,5-dimethylthiazol-2-yl)-2,5-diphenyl tetrazolium bromide (MTT) assay was carried out on MCF-7 and HCT116 cells treated with the individual compounds and the six possible combinations of a 4,6-diamino-1,2-dihydro-1,3,5-triazine with a chalcone at a 1:1 M ratio. Cell viability after 72 h of incubation with the compounds was then assessed.

The dose–effect curves of the 4,6-diamino-1,2-dihydro-1,3,5-triazines **T1**-**T2** and chalcones **C1**–**C3** were observed to be markedly different from each other. At high doses, the maximum decrease in cell viability effected by **T1**-**T2** was approximately 50%, whereas **C1**–**C3** decreased cell viability by 100%. Additionally, the Hill slope of the dose–effect curves of **T1**-**T2** was ~1, whereas the Hill slope of **C1**–**C3** ranged from ~2 to 4. Synergy analysis using mathematical models such as the Bliss independence model [22], Loewe additivity model [23] and the median effect principle by Chou and Talalay [24] was unsuitable, since an underlying assumption for these models is that the individual drugs will give rise to equal maximal effects. Modified equations based on the Loewe additivity model have been derived by Grabovsky and Tallarida [25] for cases whereby the two individual drugs produce different maximal effects. However, these equations assume that Hill slope = 1 for both drugs. In the absence of an appropriate mathematical model, we therefore adopted the concept of cooperative effect synergy, which is simply defined as an increase in the effect of the drug combination over the agents alone. In a review of synergy methodologies, Geary recommended this simpler definition of synergy because it avoids mathematical difficulties, is easily applicable, meets FDA criteria for evaluation of combination therapies, and is adequate for basic discovery and clinical research [26].

In order to determine whether the drug combinations showed a better effect than their individual components, their dose–effect curves were plotted and compared. Dose-effect curves on MCF-7 and HCT116 cells are shown in Figs. 2 and 3 respectively. In the dihydrotriazine-chalcone combinations **T1** + **C1** and **T1** + **C3**, when used at low-to-moderate concentrations of 1.5–15 μM, both 4,6-diamino-1,2-dihydro-1,3,5-triazine and chalcone components in the combination contributed to a stronger anti-proliferative effect that resulted in a greater reduction in cell viability in comparison to the decrease in cell viability brought about by treatment with the individual components (Figs. 2A, C, 3A, C). Hence, at these concentrations, a small cooperative effect was observed between **T1** and **C1** or **C3**. However, at higher concentrations, the dose–effect

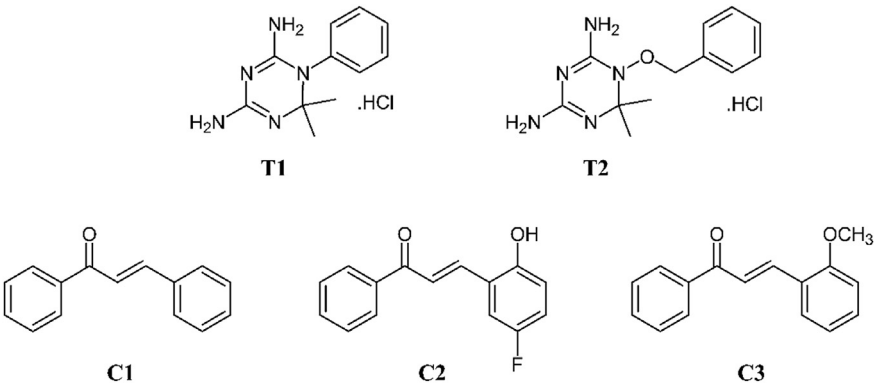


**Fig. 1.** Structures of the 4,6-diamino-1,2-dihydro-1,3,5-triazines **T1**-**T2** and the chalcones **C1**–**C3** used in the combination study.

**Table 1**
Recombinant human DHFR inhibitory activity and anti-proliferative activity of dihydrotriazines **T1** and **T2** on MCF-7 and HCT116 cells.

| Compound | DHFR $IC_{50}$ (μM) | Anti-proliferative activity | | | |
|---|---|---|---|---|---|
| | | MCF-7 cells | | HCT116 cells | |
| | | $GI_{50}$ (μM) | $LC_{50}$ (μM) | $GI_{50}$ (μM) | $LC_{50}$ (μM) |
| **T1** | 9.36 ± 0.70 | 12.7 ± 2.6 | >100 | 6.6 ± 1.8 | >100 |
| **T2** | 0.43 ± 0.03 | 2.5 ± 0.9 | >100 | 0.24 ± 0.11 | >100 |

$IC_{50}$, $GI_{50}$ and $LC_{50}$ values are presented as means ± SD from 3 independent experiments.

in enhanced anti-proliferative activities at low-to-moderate concentrations of up to ~10 μM. Thus, it should be noted that dihydrotriazine-chalcone combinations were still advantageous when compared to treatment with 4,6-diamino-1,2-dihydro-1,3,5-triazine or chalcone alone. In general, at lower concentrations, the combinations had the advantage of greater growth inhibitory activity when compared to the individual chalcones. At higher concentrations, the combinations demonstrated cell kill that was not observed with the use of 4,6-diamino-1,2-dihydro-1,3,5-triazines alone. Hence, these observations have laid the basis that supports

**Table 2**
Rat liver TrxR inhibitory activity and anti-proliferative activity of chalcones **C1**–**C3** on MCF-7 and HCT-116 cells.

| Compound | TrxR $IC_{50}$ (μM) (60 min incubation) | Anti-proliferative activity | | | |
|---|---|---|---|---|---|
| | | MCF-7 cells | | HCT116 cells | |
| | | $GI_{50}$ (μM) | $LC_{50}$ (μM) | $GI_{50}$ (μM) | $LC_{50}$ (μM) |
| **C1** | 10.8 ± 0.3 | 12.4 ± 2.0 | 30.7 ± 5.1 | 15.7 ± 2.2 | 22.5 ± 1.5 |
| **C2** | 2.6 ± 0.1 | 5.0 ± 0.4 | 17.0 ± 2.5 | 3.8 ± 0.7 | 6.5 ± 0.3 |
| **C3** | 24.5 ± 5.5 | 11.2 ± 2.9 | 42.7 ± 7.3 | 13.5 ± 0.6 | 26.6 ± 4.7 |

$IC_{50}$, $GI_{50}$ and $LC_{50}$ values are presented as means ± SD from 3 independent experiments.

curve of the combination overlapped with that of the individual chalcone (**C1**, **C3**), suggesting that the antiproliferative effect of the combinations was predominantly due to the chalcone component. As for the combination of **T1** + **C2**, the dose–effect curve was observed to overlap with that of **C2** across all concentrations (Figs. 2B and 3B), which indicated that the antiproliferative activity of the **T1** + **C2** combination was predominantly due to **C2** that possessed markedly stronger anti-proliferative profile than that of **T1**. Moving on to the dihydrotriazine-chalcone combinations **T2** + **C1**, **T2** + **C2** and **T2** + **C3**, at low-to-moderate concentrations (up to ~10 μM), the dose–effect curves of the combinations overlapped with that of **T2**, while at higher concentrations (>10 μM), the dose–effect curves overlapped with that of the individual chalcones (**C1**, **C2**, **C3**) (Figs. 2D–F, 3D–F). This had indicated that at low-to-moderate concentrations, the combinations were no better than **T2** alone while at higher concentrations, the combinations were no better than the respective chalcones alone. Therefore, taken together, results obtained had indicated that treatment with 4,6-diamino-1,2-dihydro-1,3,5-triazine-chalcone combinations at a 1:1 M ratio did not produce strong synergy.

Nonetheless, despite the general lack of synergistic antiproliferative activities of the 4,6-diamino-1,2-dihydro-1,3,5-triazine-chalcone combination, it was notable that the combination of **T1** and **C1**/**C3** displayed cooperative effects that culminated the notion that incorporation of the 4-6-diamino-1,2-dihydro-1,3,5-triazine and chalcone scaffolds into a single chemical entity would potentially result in novel compounds possessing stronger antiproliferative profiles than their parent (dihydrotriazine/chalcone) compounds.

### 2.2. Merged dihydrotriazine-chalcone compounds

#### 2.2.1. Design and synthesis of merged dihydrotriazine-chalcone compounds

2,2-Dimethyl-1-phenyl-1,2-dihydro-1,3,5-triazine-4,6-diamine HCl **T1** and unsubstituted chalcone **C1** were used as starting point for the design of novel merged dihydrotriazine-chalcone compounds. **T1** and **C1** were chosen due to their (1) potent inhibitory activities against DHFR and TrxR respectively, (2) strong antiproliferative activity in the μM range of concentrations, and (3) cooperative effect observed when used together as combination treatment. Additionally, **T1** and **C1** have low molecular weights of 253.7 and 208.3 respectively. Considering that designed multiple ligands are generally bulkier and more lipophilic than other drugs, thereby resulting in a poorer pharmacokinetic profile[3], it is thus advantageous that the individual scaffolds are small in size. There are three ways of joining different pharmacophores to obtain multi-targeted compounds: by conjugation, fusion and merging of the

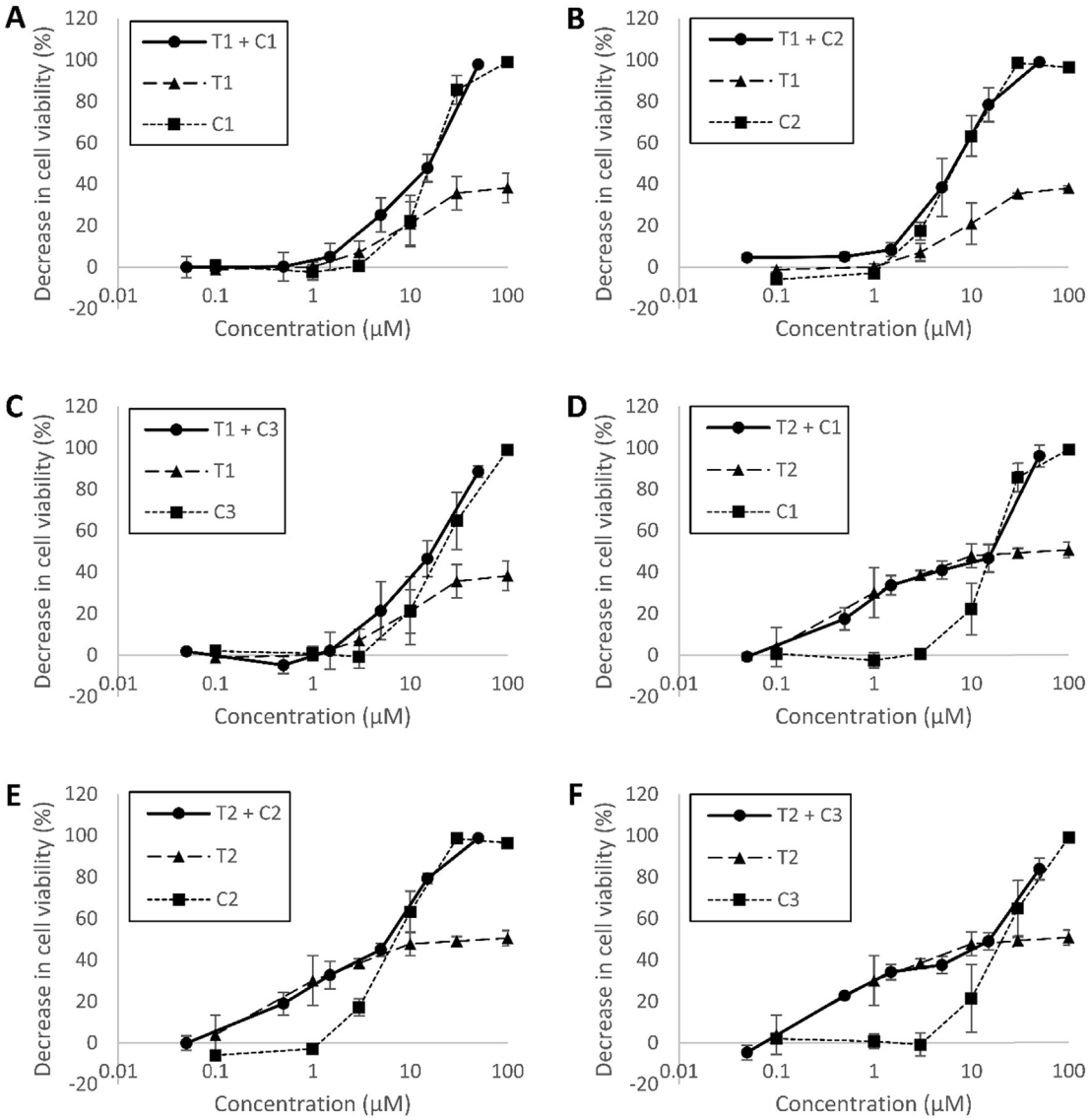


**Fig. 2.** Dose-dependent effects of 4,6-diamino-1,2-dihydro-1,3,5-triazines **T1**/**T2**, chalcones **C1**/**C2**/**C3** or their combination on viability of MCF-7 cells. MCF-7 cells were incubated with (A) **T1**, **C1** and their combination at a 1:1 M ratio, (B) **T1**, **C2** and their combination at a 1:1 M ratio, (C) **T1**, **C3** and their combination at a 1:1 M ratio, (D) **T2**, **C1** and their combination at a 1:1 M ratio, (E) **T2**, **C2** and their combination at a 1:1 M ratio, and (F) **T2**, **C3** and their combination at a 1:1 M ratio for 72 h and cell viabilities were determined using MTT assay. Concentration was plotted on a logarithmic scale. Each data point represents the average value from three independent experiments.

chemical frameworks containing the individual pharmacophores.[1] Briefly, "conjugated" compounds contain a distinct linker separating the frameworks containing the pharmacophores for each biological target whereas compounds are "fused" when the frameworks are directly connected. Finally, overlap between the pharmacophoric elements results in "merged" compounds. A common structural feature present in both **T1** and **C1** is the phenyl ring. As shown in Fig. 4, in **T1**, the phenyl ring is attached to the N1 atom of the 1,2-dihydro-1,3,5-triazine ring and **C1** contains two phenyl rings that are denoted as ring A and ring B. The phenyl rings are located in tolerant regions of both scaffolds, meaning that substitutions can be made on the phenyl rings without destroying enzyme inhibitory activity and anti-proliferative activity. Hence, the structures of **T1** and **C1** were "merged" in our effort to synthesize novel dual-target compounds against DHFR and TrxR. The chemical structures of **T1**, **C1** and the resulting merged dihydrotriazine-chalcone compounds are shown in Fig. 4: the phenyl ring attached to N1 of **T1** was merged with either ring A or ring B of **C1** at the *meta*- or *para*-position.

The synthetic route for compounds **6a** and **6b** is outlined in Scheme 1. Nitro-substituted chalcones (**3a**-**b**) (81–86% yield) were synthesized via the Claisen–Schmidt condensation reaction between acetophenone and *p*-nitrobenzaldehyde (**1**) or *m*-nitrobenzaldehyde (**2**). The nitro group was then reduced by refluxing with iron powder and ammonium chloride in an aqueous ethanolic solution to obtain amino-substituted chalcones (**4a**-**b**) (55–63% yield), which were further reacted with cyanoguanidine in the presence of concentrated HCl to form compounds **5a**-**b** (72–75% yield). Finally, ring closure of these compounds with acetone in the presence of concentrated HCl afforded the target compounds **6a** and **6b** (40–55% yield). Ring closure to obtain **6a** was achieved at room temperature, whereas ring closure to obtain **6b** required microwave-assisted synthesis at 90 °C for 1 h. The final products were purified by recrystallization from ethanol/water.

The synthetic route for compounds **11a** and **11b** is outlined in Scheme 2. Attempts to synthesize 3'-nitrochalcone and 4'-

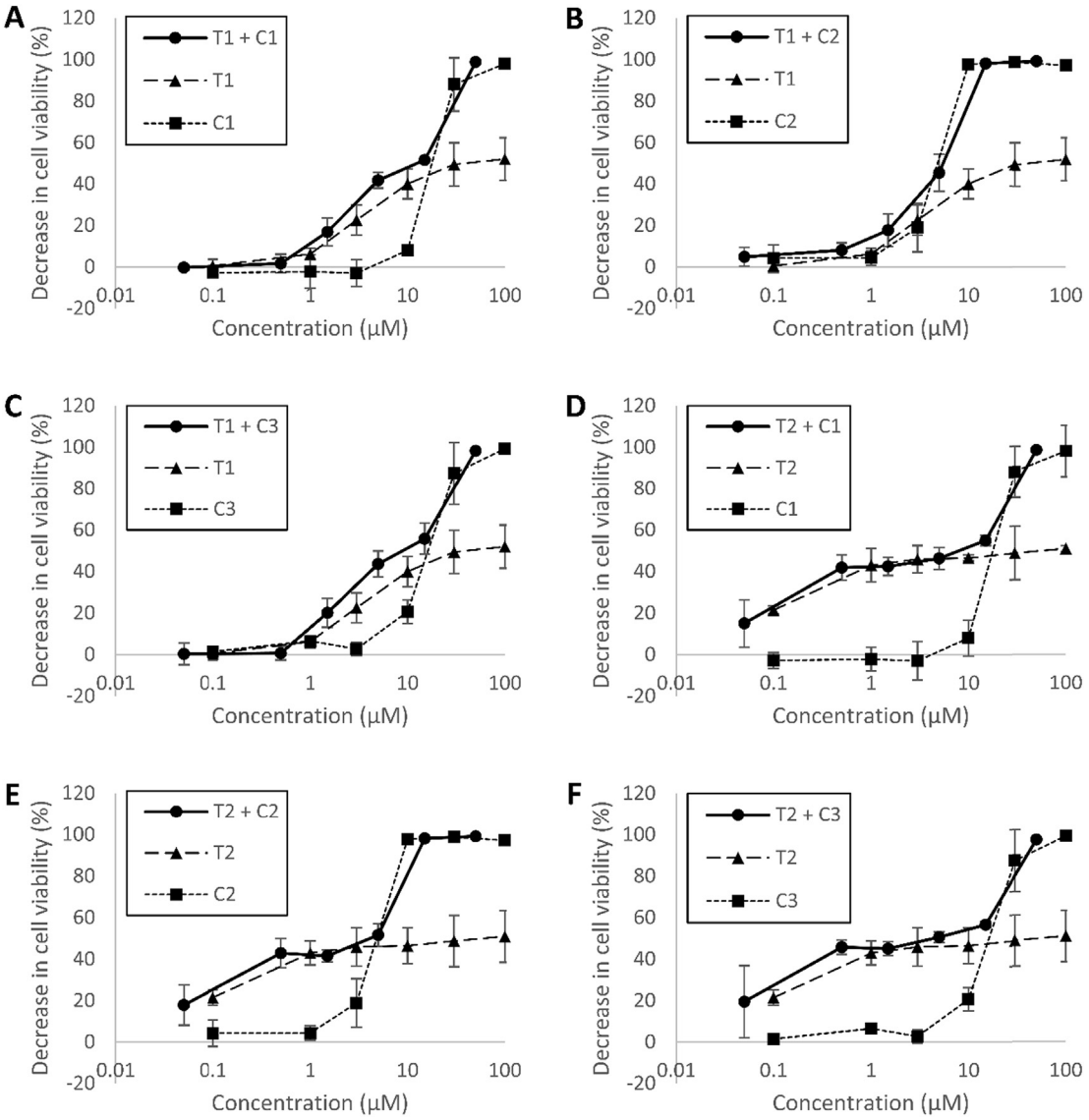


**Fig. 3.** Dose-dependent effects of 4,6-diamino-1,2-dihydro-1,3,5-triazines **T1**/**T2**, chalcones **C1**/**C2**/**C3** or their combination on viability of HCT116 cells. HCT116 cells were incubated with (A) **T1**, **C1** and their combination at a 1:1 M ratio, (B) **T1**, **C2** and their combination at a 1:1 M ratio, (C) **T1**, **C3** and their combination at a 1:1 M ratio, (D) **T2**, **C1** and their combination at a 1:1 M ratio, (E) **T2**, **C2** and their combination at a 1:1 M ratio, and (F) **T2**, **C3** and their combination at a 1:1 M ratio for 72 h and cell viabilities were determined using MTT assay. Concentration was plotted on a logarithmic scale. Each data point represents the average value from three independent experiments.

nitrochalcone by sodium hydroxide-catalyzed condensation resulted in poor yields. Hence, Boc-protection was used instead to obtain the desired amino-substituted chalcones (**9a**-**b**). *P*-aminoacetophenone (**7**) or *m*-aminoacetophenone (**8**) was Boc-protected, reacted with benzaldehyde in the presence of sodium hydroxide as a base catalyst, and then Boc-deprotected to yield **9a**-**b** (62–90% yield). These amino-substituted chalcones were reacted with cyanoguanidine in the presence of concentrated HCl to form compounds **10a**-**b**. When this reaction was carried out under reflux conditions, no product was formed. Hence, the temperature was increased to 120 °C using microwave-assisted synthesis. The reaction was found to be incomplete after 15 min and gave **10a**-**b** in low yields of 8–10%, but longer reaction times resulted in more side-products formed (TLC). Ring closure of these compounds with acetone in the presence of concentrated HCl yielded the target compounds **11a** and **11b** (53–63%). **11a** was purified by recrystallization from ethanol/acetone, while **11b** was purified using column chromatography.

### 2.2.2. *Effects of merged dihydrotriazine-chalcone compounds on in vitro DHFR and TrxR activities*

The DHFR inhibition assay was carried out using a spectrophotometric assay against recombinant human DHFR. The rate of NADPH consumption during the conversion of dihydrofolate to tetrahydrofolate by DHFR in the presence of varying concentrations of test compounds was monitored at 340 nm and calculated $IC_{50}$ values are shown in Table 3. The compounds in which **T1** was merged with ring B of **C1** (**6a** and **6b**) failed to inhibit DHFR even at a high concentration of 100 μM. Conversely, compounds in which **T1** was merged with ring A of **C1** (**11a** and **11b**) did not have DHFR inhibitory activity abrogated. Notably, merging of **T1** with ring A of **C1** at the *para*-position (**11a**) had led to a 6-fold reduction in DHFR inhibitory activity as compared to that of the parent dihydrotriazine **T1**. On the other hand, merging of **T1** with ring A of **C1** at the *meta*-position (**11b**) gave rise to enhancement of DHFR inhibitory activity with a 4-fold increase in potency as compared to that of **T1**.

The TrxR inhibitory activities of the test compounds were

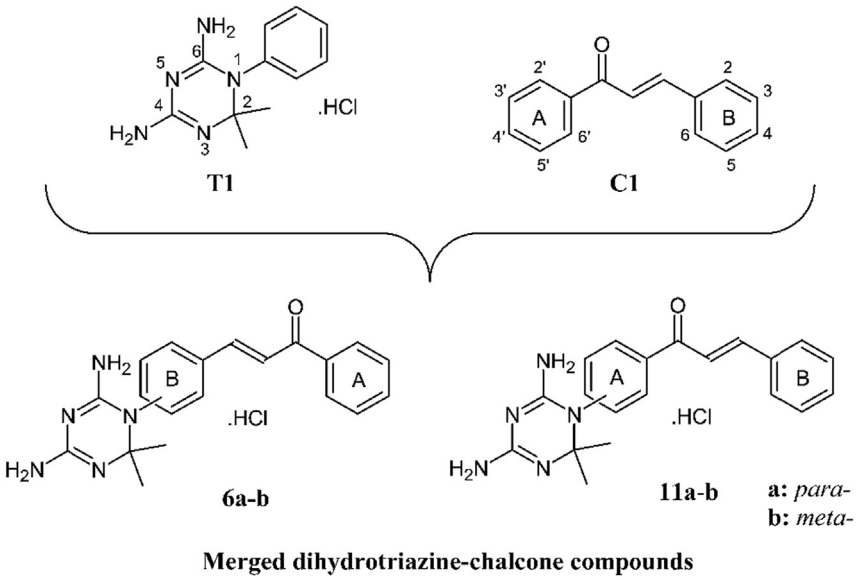


**Fig. 4.** Structures of **T1**, **C1** and merged dihydrotriazine-chalcone compounds.

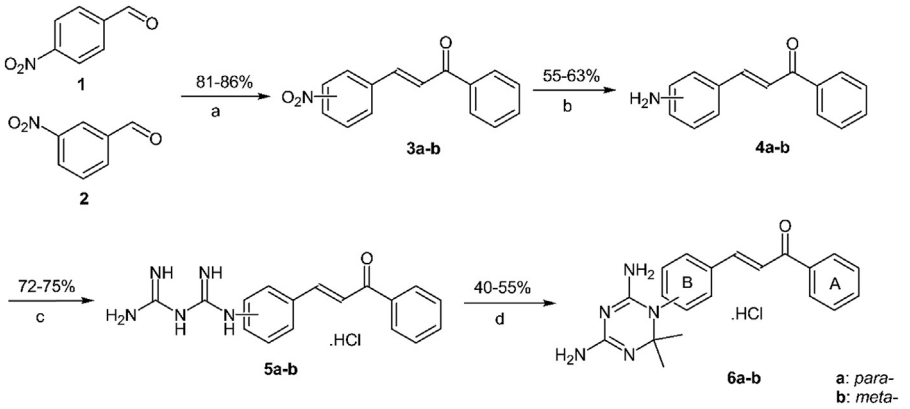


**Scheme 1.** Synthesis of compounds **6a** and **6b**. Reagents and conditions: a) acetophenone, NaOH, EtOH, $H_2O$, rt; b) Fe/$NH_4Cl$, EtOH, $H_2O$, reflux; c) cyanoguanidine, conc. HCl, acetonitrile, reflux; d) acetone, conc. HCl, EtOH, rt for **6a**/microwave at 90 °C for 1 h for **6b**.

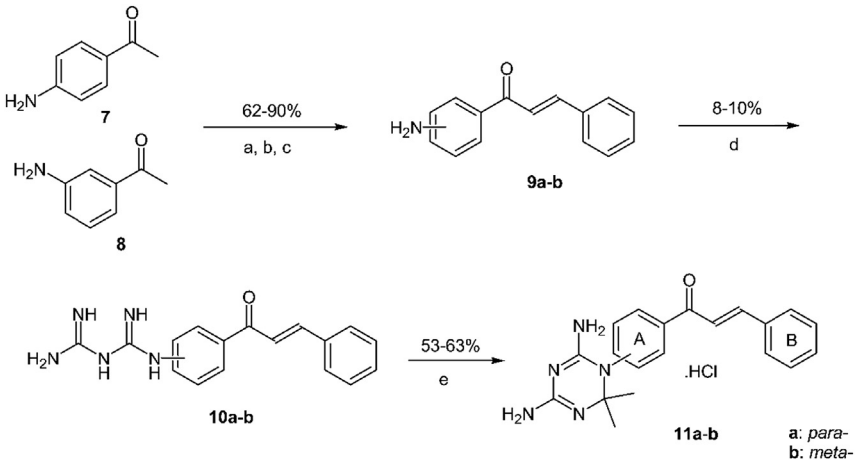


**Scheme 2.** Synthesis of compounds **11a** and **11b**. Reagents and conditions: a) $Boc_2O$, dioxane, rt; b) benzaldehyde, NaOH, EtOH, $H_2O$, rt; c) TFA, rt; d) cyanoguanidine, conc. HCl, EtOH, microwave at 120 °C for 15 min; e) acetone, conc. HCl, rt.

determined using the 5.5'-dithiobis-(2-nitrobenzoic acid) (DTNB) assay following 30 and 60 min incubation of the compounds with

**Table 3**
$IC_{50}$ values of **T1**, **C1** and merged dihydrotriazine-chalcone compounds **6a**-**b** and **11a**-**b** against recombinant human DHFR and rat liver TrxR.

| Compound | DHFR $IC_{50}$ (μM) | TrxR $IC_{50}$ (μM) | |
|---|---|---|---|
| | | 30 min Incubation | 60 min Incubation |
| **6a** | >100 | 6.2 ± 2.0 | 5.4 ± 1.1 |
| **6b** | >100 | 7.2 ± 3.5 | 4.2 ± 1.3 |
| **11a** | 56.4 ± 15.3 | 18.6 ± 5.0 | 12.6 ± 3.0 |
| **11b** | 2.4 ± 0.5 | 15.7 ± 3.9 | 10.1 ± 2.3 |
| **T1** | 9.4 ± 0.7 | >100 | >100 |
| **C1** | >100 | 46.4 ± 9.9 | 26.7 ± 4.3 |
| **MTX** | **0.0079 ± 0.0002** | **>100** | **>100** |

$IC_{50}$ values are presented as means ± SD from 3 independent experiments.

TrxR isolated from rat liver. DTNB is a substrate of TrxR that was reduced to 2-nitro-5-thiobenzoate (TNB) in the presence of NADPH. Rate of production of TNB, reflective of TrxR activity, was monitored at 412 nm and calculated $IC_{50}$ values are shown in Table 3. All of the dihydrotriazine-chalcone hybrids exhibited more potent TrxR inhibitory activity as compared to those of the parent chalcone **C1**. Merging of **T1** to ring B of **C1** (**6a**-**b**) resulted in a greater improvement in TrxR inhibitory activity as compared to merging of **T1** to ring A of **C1** (**11a**-**b**) by 2–3 times.

A possible explanation for the improvement in TrxR inhibitory activity of the merged dihydrotriazine-chalcone compounds over **C1** was the increased reactivity of the α,β-unsaturated carbonyl moiety, which had been postulated as the reactive pharmacophoric motif in chalcones to react with the nucleophilic Sec residue within the C-terminal active site of the TrxR enzyme. At physiological pH, the N-3 atom of the 4,6-diamino-1,2-dihydro-1,3,5-triazine ring is protonated. The resulting positive charge can be delocalized over the N-3 atom, 4-amino group, 6-amino group and N-1 atom of the ring. Since the N-1 atom of the dihydrotriazine ring is directly attached to either ring A or ring B of the chalcone, the positively-charged dihydrotriazine ring may exert an electron-withdrawing effect on the chalcone. This intensifies the $\delta+$ charge on the β-carbon atom of the α,β-unsaturated carbonyl moiety, thereby increasing its reactivity. This effect is stronger when the dihydrotriazine ring is attached to ring B than when attached to ring A, which might explain the greater TrxR inhibitory activities of compounds **6a** and **6b** as compared to those of **11a** and **11b**.

### 2.2.3. Molecular docking of compound 11b with DHFR and TrxR

In order to investigate the binding mode of the dihydrotriazine-chalcone linked compounds to DHFR and TrxR, compound **11b** was selected for molecular docking experiments as it showed good *in vitro* inhibitory activity against both DHFR and TrxR. The method protomol generation by ligand was selected for the molecular docking studies on compound **11b** against DHFR using Surflex-dock. Human DHFR complexed with MTX (PDB: 1U72) was obtained from protein data bank (PDB) and modified for the docking experiment. During protein preparation, the co-crystalized ligand was first removed from the structure together with the water molecules. H atoms were then added and side chains were fixed. Fig. 5A depicts the docking of compound **11b** into the active site of human DHFR. As expected, compound **11b** binds to the active site with a similar binding mode compared to MTX [27]. In this binding mode, **11b** demonstrated good binding to DHFR with a high docking score of 7.17 (-log $K_d$). Several hydrogen bonds were observed between compound **11b** and the crucial amino acid residues Val115 (N–H···O: 2.037 Å), Ile7 (N–H···O, 2.167 Å), Glu30 (N–H···OE2, 2.256 Å), and Ser59 (O···H–O, 2.090 Å). Compound **11b** was also revealed to be involved in strong hydrophobic interactions at the active site with the hydrophobic residues such as Ile7, Val8, Phe31, Phe34, Pro61 and Val115 (Fig. 5B).

Molecular docking was also performed for compound **11b** against the predominant cytosolic isoform of TrxR, namely TrxR1, through protomol generation by residues residing in the enzyme's C-terminal active site. The residues involved with binding are Ser495, Gly496, Cys497, Sec498, Ile478, Glu477, His472 and Phe406. The crystal structure of rat TrxR1 (PDB: 3EAN) was taken from PDB, and modified for docking calculations. During protein preparation, water molecules were removed, H atoms were added and side chains were fixed. Fig. 6A and B shows respectively the docking of compound **11b** into the C-terminal active site of TrxR1 and the interaction between compound **11b** and the hydrophobic surface proximal to the active site of TrxR1. The docking score for this interaction was found to be 4.33; the low docking score was likely due to the inability of Surflex-dock to recognize covalent interactions in its calculation. Nevertheless, the docking results show a potential hydrogen bond formation between O of the carbonyl group of compound **11b** and the side chain amide group of Gln494 (O···H–N, 1.991 Å). In addition, non-polar amino acid residues Phe406, Trp407, Gly496 and Ile478 at the C-terminal tail of TrxR were found to be involved in hydrophobic interactions with compound **11b**. In summary, taking together the results obtained from the molecular docking work that was performed, compound 11b was shown to possess rational binding modes to both DHFR and TrxR.

### 2.2.4. Antiproliferative activities of merged dihydrotriazine-chalcone compounds

Based on the obtained $GI_{50}$ and $LC_{50}$ values presented in Table 4, one notable observation was that all of the merged dihydrotriazine-chalcone compounds only exhibited growth inhibitory activities but cytotoxic effects were generally lacking ($LC_{50}$ values greater than 100 μM). Merging of **T1** with **C1** at the *para*-position of ring A (**11a**) or ring B (**6a**) apparently produced good growth inhibitory potencies. Conversely, merging of **T1** with **C1** at the *meta*-position of ring A (**11b**) or ring B (**6b**) was detrimental; the resulting merged compounds possessed poor growth inhibitory activities against MCF-7 and HCT116 cells (Table 4). A second notable observation was the poor correlation between the anti-proliferative activities and *in vitro* DHFR and TrxR inhibitory activities of the merged compounds; the order of growth inhibitory potencies displayed by the merged compounds did not correspond to a similar order of inhibitory potencies against DHFR and TrxR. Taking together the findings made of the anti-proliferative properties, as well as DHFR and TrxR inhibitory properties of the merged compounds, the following inferences were made: firstly, the merged dihydrotriazine-chalcone compounds, particularly **11a** and **11b**, brought about both DHFR and TrxR inhibition in an *in vitro* setting, which not only demonstrated the feasibility of synthetically combining a DHFR-targeting triazine and TrxR-targeting chalcone pharmacophore into a single novel molecule, but also provided experimental evidence that the resulting compounds indeed possessed inhibitory character against both molecular targets of interest. Secondly, the weak cell-killing efficacies among the merged dihydrotriazine-chalcone compounds, as well as a poor correlation between their anti-proliferative activities and *in vitro* DHFR and TrxR inhibitory activities, had indicated that the current "merged compound" design approach that involved structural combination of the dihydrotriazine and chalcone scaffold through an overlap of the common phenyl ring attached to N1 atom of the dihydrotriazine ring could be improved on so as to produce novel molecules that possessed potent anti-proliferative profiles correlated to strong DHFR and TrxR inhibitory activities.

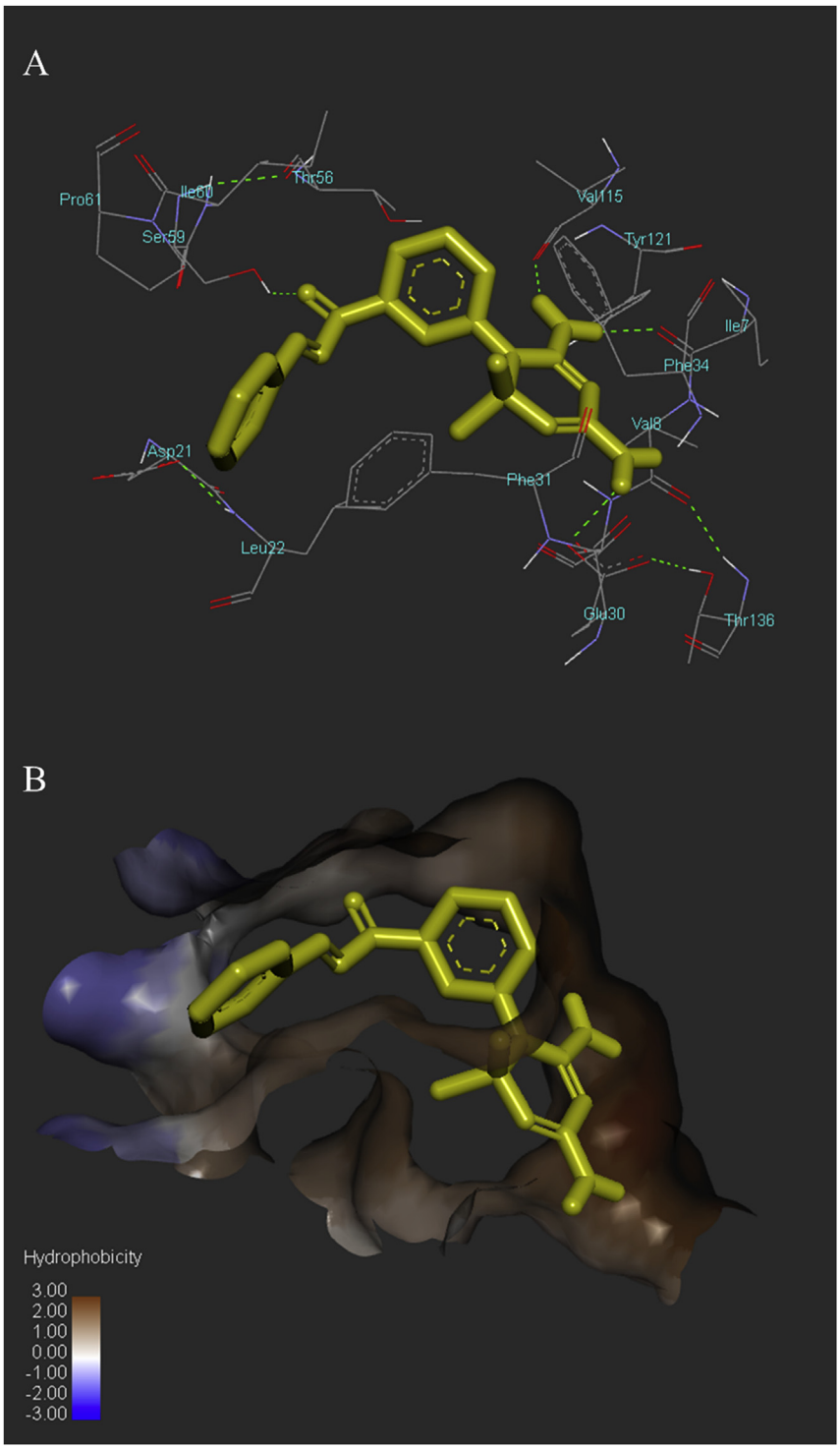


**Fig. 5.** Molecular docking of compound **11 b** at the active site of human DHFR using Surflex-Dock. (A) Selected docking pose of compound **11 b** at the active site of human DHFR that gave a high docking score. (B) Visualization of compound **11b** interacting with the hydrophobic residues at the active site of DHFR.

## 3. Conclusion

To exploit the possibility of harnessing the combined benefits of simultaneous inhibition of molecular targets DHFR and TrxR so as to achieve enhanced anti-tumor outcomes, two approaches had been examined in this study. The approach involving the combined treatment of MCF-7 and HCT116 cells with 4,6-diamino-1,2-dihydro-1,3,5-triazines and chalcones at a 1:1 M ratio resulted in synergy only at relatively low concentrations. In the approach involving structural combination of the 4,6-diamino-1,2-dihydro-1,3,5-triazine and chalcone scaffold into a single molecule (through an overlap of the common phenyl ring attached to N1 atom of the dihydrotriazine ring), four "merged" dihydrotriazine-chalcone compounds were designed and synthesized. Two of the compounds, **11a** and **11b**, were found to possess both *in vitro* DHFR and TrxR inhibitory activities, which indicated the feasibility of

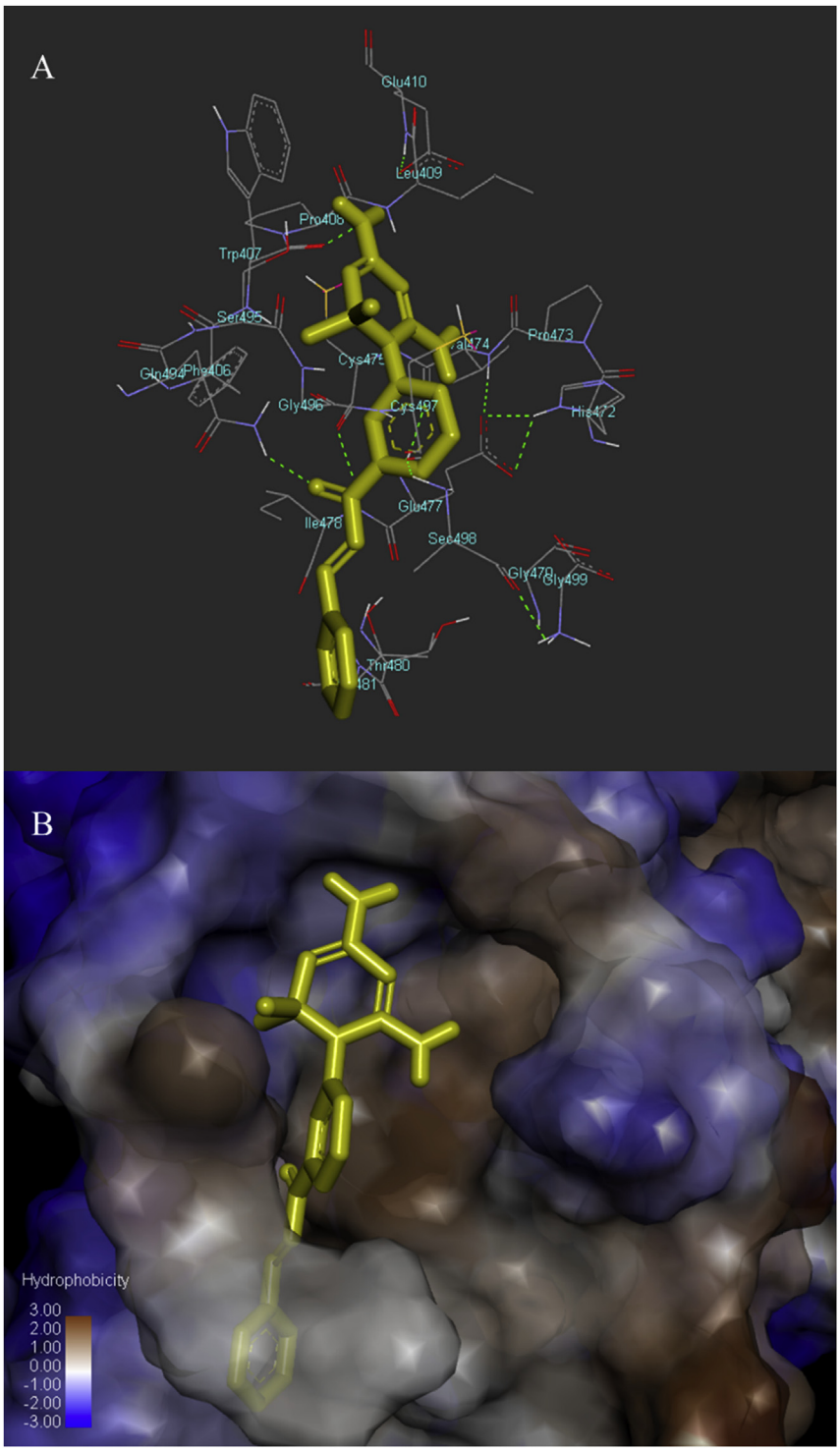


**Fig. 6.** Molecular docking of compound **11 b** at the C-terminal active site of rat TrxR1 using Surflex-Dock. (A) Selected docking pose of compound **11 b** at the C-terminal active site of rat TrxR1. (B) Visualization of compound **11b** interacting with the hydrophobic surface of the C-terminal active site of rat TrxR1.

producing a single chemical entity that could result in simultaneous inhibition of DHFR and TrxR. However, the synthesized merged compounds only exhibited growth inhibitory activities like their parent dihydrotriazine component, and lacked cytotoxic efficacies like their parent chalcone component. In addition, their anti-proliferative activities did not correlate with their DHFR and TrxR enzyme inhibitory activities. Taken together, the findings of this proof-of-concept study, while indicative of the synthetic feasibility of producing a single chemical entity that could result in simultaneous inhibition of DHFR and TrxR, had exposed the sub-optimal structural design of combination of the two pharmacophores in a single chemical entity. Other synthetic ways of deriving compounds using the "designed multiple ligand" approach, such as conjugation or fusion of the chemical frameworks containing the

**Table 4**
Antiproliferative activity of **T1**, **C1** and merged dihydrotriazine-chalcone compounds **6a-b** and **11a-b** against MCF-7 and HCT116 cancer cell lines.

| Compound | MCF-7 cells | | HCT116 cells | |
|---|---|---|---|---|
| | $GI_{50}$ (μM) | $LC_{50}$ (μM) | $GI_{50}$ (μM) | $LC_{50}$ (μM) |
| **6a** | 2.0 ± 0.6 | >100 | 1.4 ± 0.2 | >100 |
| **6b** | 51.5 ± 12.9 | >100 | >100 | >100 |
| **11a** | 3.0 ± 0.6 | >100 | 10.7 ± 2.7 | >100 |
| **11b** | 34.4 ± 2.0 | >100 | 74.4 ± 4.5 | >100 |
| **T1** | 12.7 ± 2.6 | >100 | 6.6 ± 1.8 | >100 |
| **C1** | 12.4 ± 2.0 | 30.7 ± 5.1 | 15.7 ± 2.2 | 22.5 ± 1.5 |
| **MTX** | 0.024 ± 0.007 | >100 | 0.015 ± 0.001 | >100 |

$GI_{50}$ and $LC_{50}$ values are presented as means ± SD from 3 independent experiments.

individual DHFR- and TrxR-targeting pharmacophores will need to be explored.

## 4. Experimental

### 4.1. General conditions for organic synthesis

All reagents were purchased from Sigma–Aldrich, Tokyo Chemical Industry, Alfa Aesar, or Merck and were used directly without any purification. Microwave reactions were carried out using a CEM Discover® SP System. Thin layer chromatography (TLC) was performed using silica gel-coated aluminum plates with fluorescent indicator and visualized with ultraviolet light at 254 nm. Melting points were determined using a Gallenkamp melting point apparatus and were uncorrected. $^1$H NMR and $^{13}$C NMR spectra were recorded on a Bruker Ultrashield™ 400 Plus NMR spectrometer. Chemical shift values ($\delta$) were expressed as parts per million (ppm) relative to tetramethylsilane as the internal standard. Electrospray ionization mass spectrometry (ESI-MS) was recorded on an AB SCIEX API 2000 Q Trap mass spectrometer. High performance liquid chromatography (HPLC) was performed for purity checking using Agilent 1100 Series HPLC on a Lichrosorb 10 RP-18 250 × 4.0 mm 10 μm column.

### 4.2. (2E)-3-[4-(4,6-diamino-2,2,dimethyl-1,3,5-triazin-1(2H)-yl) phenyl]-1-phenylprop-2-en-1-one hydrochloride (**6a**)

To a solution of **5a** (1.15 g, 3.34 mmol) in 10 ml acetone and 10 ml ethanol, 0.45 ml of concentrated HCl solution was added and the reaction mixture was stirred at room temperature for 3 days. The solvent was removed under reduced pressure and the residual solid was purified by recrystallization from ethanol/water to give **6a** as orange crystals, 0.706 g, yield 55.1%. mp: 208–210 °C. $^1$H NMR (400 MHz, DMSO-$d_6$) $\delta$ 8.76 (s, 1H, NH), 8.16–8.13 (m, 2H), 8.03 (d, 2H, J = 8.4 Hz), 7.97 (d, 1H, J = 15.6 Hz), 7.80 (d, 1H, J = 15.6 Hz), 7.72 (tt, 1H, J = 7.4, 1.5 Hz), 7.62 (t, 2H, J = 7.6 Hz), 7.53 (br s, 3H, NH), 7.46 (d, 2H, J = 8.4 Hz), 6.47 (br s, 1H, NH), 1.40 (s, 6H). $^{13}$C NMR (100 MHz, DMSO-d6) $\delta$ 189.1, 157.7, 157.0, 142.6, 137.3, 136.5, 135.7, 133.2, 130.4, 128.8, 128.5, 123.4, 69.7, 27.2. Purity: 99.2%, HPLC $t_R$ = 3.24 min. ESI-MS $m/z$ 348.3 $(M+1)^+$.

### 4.3. (2E)-3-[3-(4,6-diamino-2,2,dimethyl-1,3,5-triazin-1(2H)-yl) phenyl]-1-phenylprop-2-en-1-one hydrochloride (**6b**)

To a solution of **5b** (0.44 g, 1.28 mmol) in 3.5 ml acetone and 1.5 ml ethanol, 0.2 ml of concentrated HCl solution was added and the reaction mixture was heated using microwave-assisted synthesis at 90 °C for 1 h. The solvent was removed under reduced pressure and the residual solid was purified by recrystallization from ethanol to give **6b** as brown crystals, 0.199 g, yield 40.4%. mp: 273 °C (decomposed). $^1$H NMR (400 MHz, DMSO-$d_6$) $\delta$ 9.86 (s, 1H, NH), 8.88 (s, 1H, NH), 8.72 (s, 1H, NH), 8.15–8.12 (m, 2H), 7.91–7.69 (m, 5H), 7.77 (br s, 1H, NH), 7.63–7.59 (m, 2H), 7.55–7.53 (m, 1H), 7.47 (t, 1H, J = 7.8 Hz), 7.18 (br s, 1H, NH), 1.49 (s, 6H). $^{13}$C NMR (100 MHz, DMSO-d6) $\delta$ 189.2, 157.5, 155.2, 143.6, 137.9, 137.4, 135.3, 133.1, 129.3, 128.7, 128.4, 124.14, 124.09, 122.8, 122.6, 64.8, 28.9. Purity: 99.6%, HPLC $t_R$ = 3.55 min. ESI-MS $m/z$ 348.1 $(M+1)^+$.

### 4.4. (2E)-1-[4-(4,6-diamino-2,2,dimethyl-1,3,5-triazin-1(2H)-yl) phenyl]-3-phenylprop-2-en-1-one hydrochloride (**11a**)

To a solution of **10a** (0.15 g, 0.42 mmol) in 1 ml acetone and 1 ml ethanol, 0.1 ml of concentrated HCl solution was added and the reaction mixture was stirred at room temperature for 3 days. The solvent was removed under reduced pressure and the residual solid was purified by recrystallization from ethanol/acetone to give **11a** as a yellow solid, 0.086 g, yield 53.2%. mp: 175–177 °C. $^1$H NMR (400 MHz, DMSO-$d_6$) $\delta$ 9.22 (s, 1H, NH), 8.30 (d, 2H, J = 8.4 Hz), 8.02–7.78 (m, 4H), 7.60 (d, 2H, J = 8.4 Hz), 7.55 (br s, 3H, NH), 7.49–7.48 (m, 3H), 6.53 (br s, 1H), 1.40 (s, 6H). $^{13}$C NMR (100 MHz, DMSO-d6) $\delta$ 188.6, 157.5, 156.8, 144.7, 138.8, 138.1, 134.4, 130.8, 130.5, 130.3, 128.94, 128.87, 121.8, 69.8, 27.2. Purity: 99.3%, HPLC $t_R$ = 4.39 min. ESI-MS $m/z$ 348.3 $(M+1)^+$.

### 4.5. (2E)-1-[3-(4,6-diamino-2,2,dimethyl-1,3,5-triazin-1(2H)-yl) phenyl]-3-phenylprop-2-en-1-one hydrochloride (**11b**)

To a solution of **10b** (0.24 g, 0.69 mmol) in 1 ml acetone and 1 ml ethanol, 0.1 ml of concentrated HCl solution was added and the reaction mixture was stirred at room temperature for 9 days. The solvent was removed under reduced pressure and the residual brown sticky substance was purified by column chromatography to give **11b** as a light brown solid, 0.168 g, yield 63.3%. mp: 174–176 °C. $^1$H NMR (400 MHz, DMSO-$d_6$) $\delta$ 9.36 (s, 1H, NH), 8.29 (d, 1H, J = 7.2 Hz), 8.17 (s, 1H), 8.02–7.92 (m, 3H), 7.83–7.70 (m, 3H), 7.50–7.48 (m, 3H), 7.43 (br s, 3H, NH), 6.51 (br s, 1H, NH), 1.40 (s, 6H). $^{13}$C NMR (100 MHz, DMSO-d6) $\delta$ 188.3, 157.7, 157.1, 144.8, 139.2, 135.3, 134.6, 134.5, 130.8, 130.6, 130.1, 129.6, 129.0, 128.8, 121.7, 69.7, 27.3, 27.2. Purity: 99.7%, HPLC $t_R$ = 4.30 min. ESI-MS $m/z$ 348.2 $(M+1)^+$.

### 4.6. In vitro DHFR inhibiton assay

To 1 ml of solution containing 50 μM dihydrofolate (DHF), 60 μM NADPH, 0.15 M phosphate buffer (pH 7), 1.5 × $10^{-3}$ units of recombinant human DHFR (Sigma–Aldrich) in a 1-ml quartz cuvette, test compounds dissolved in DMSO vechicle were added to achieve final concentrations over the range of 0.01–100 μM. Upon addition of the compounds, the rate of consumption of NADPH during the conversion of DHF to tetrahydrofolate (THF) was monitored. Absorbance readings were taken at 340 nm every 30 s over 6 min using a Hitachi U-1900 UV/visible spectrophotometer. The assay was carried out at room temperature. A graph of absorbance readings versus time was plotted and the linear slope of the graph represents the rate of reaction. The percentage inhibition at each concentration of inhibitor was calculated using the following formula:

$$\text{Activity } (\%) = \frac{\text{Slope}_{\text{compound}} - \text{Slope}_{\text{blank}}}{\text{Slope}_{\text{control}} - \text{Slope}_{\text{blank}}} \times 100$$

$$\text{Inhibition } (\%) = 100 - \text{Activity}$$

where $\text{Slope}_{\text{compound}}$ is the slope of the graph for solutions

containing DHFR, test compound, NADPH and DHF; $Slope_{control}$ is the slope of the graph for solutions containing DHFR, NADPH and DHF; while $Slope_{blank}$ is the slope of the graph for solutions containing NADPH and DHF only. Graphs of percentage inhibition against logarithmic concentration were plotted for each compound and $IC_{50}$ values were calculated using GraphPad Prism Version 5.01.

### 4.7. In vitro TrxR inhibition assay (DTNB reduction assay)

In 96-well plates, test compounds of 1–100 μM were incubated with 2.1 units/ml of rat liver TrxR and 200 μM of NADPH in a volume of 100 μl of 50 mM Tris–HCl and 1 mM EDTA, pH 7.5 (TE buffer) at room temperature for 30 min or 60 min. A volume of 100 μl of TE buffer containing 5 mM of DTNB and 200 μM NADPH was added (final concentrations: 2.5 mM DTNB, 200 μM NADPH) and the increase in absorbance at 412 nm was measured over the initial 2 min with a VersaMax Microplate Reader (Molecular Devices). Maximal velocity ($V_{max}$) values were obtained from the linear portion of the absorbance-over-time curve. TrxR activity was calculated as a percentage of enzyme activity as compared to that of vehicle-treated sample using the formula:

$$\text{Activity } (\%) = \frac{V_{\text{max compound}}}{V_{\text{max control}}} \times 100$$

Graphs of percentage activity against logarithmic concentration were plotted for each compound and $IC_{50}$ values were calculated using GraphPad Prism Version 5.01.

### 4.8. Molecular docking studies

Molecular docking of compound **11b** was conducted using the Surflex-Dock module [28,29] in SYBYL–X 1.1 (Tripos associate Inc., St. Louis, MO, USA) to evaluate the possible binding poses of the compound at the binding sites of human DHFR and rat TrxR1. The 3D structure of **11b** was minimized in SYBYL-X 1.1. The partial atomic charge was calculated by the Gasteiger Huckel method and energy minimization was performed using the Tripos force field with a distance-dependent dielectric and the Powell conjugate gradient algorithm convergence criteria. The 3D human DHFR structure PDB ID 1U72 (resolution of 1.90 Å) and rat TrxR1 structure PDB ID 3EAN (resolution of 2.75 Å) were obtained from the Protein Data Bank. Water molecules co-crystallized with protein were removed from the original 3D structure, hydrogen atoms were added and side chains were fixed during protein preparation. Surflex-Dock module docks ligands into the active site of the enzyme automatically using a protomol-based method and an empirically scoring function. The protomol in Surflex-Dock utilizes various molecular fragments, which were tessellated in the active site and optimized based on the scoring function. Docking calculation for DHFR 1U72 was performed through protomol generation by ligand, while docking calculation referring to TrxR1 3EAN was performed through protomol generation based on residues Phe405, Phe406, Trp407, His472, Val474, Gly496, Cys497, Sec498 and Gly499 in the C-terminal active site. Protomol generation parameters were threshold 0.5 and boat 0 for both enzymes. The docking score of Surflex-Dock is expressed as $-\log K_d$ to represent binding affinities which consist of hydrophobic, polar, repulsive, entropic and solvation terms. During the automated docking process, the ligand was docked into the active site in different ways, creating different poses each with a docking score. The top 20 poses of each ligand were obtained and analyzed for their interactions with the protein.

### 4.9. Cell viability assay

Breast adenocarcinoma MCF-7 and colon carcinoma HCT116 cells were maintained in RPMI 1640 medium supplemented with 10% fetal bovine serum, 100 units/ml penicillin, and 100 μg/ml streptomycin and incubated at 37 °C in a humidified atmosphere of 95% air and 5% $CO_2$. Cells were seeded into 96-well plates at a density of $1.0 \times 10^4$/well and allowed to adhere overnight. Serial dilutions of the test compounds were freshly prepared in medium from DMSO drug stocks for each assay. At the time of addition of test compounds ($T_0$) and after 72 h of incubation with test compounds, cell viability was determined by MTT assay. MTT was added into each well to achieve a final concentration of 400 μg/ml and the plates were incubated at 37 °C for 4 h. The supernatant was aspirated and the insoluble formazan product was solubilized in 150 μl of DMSO:glycine buffer, pH 10.5 (ratio 4:1). Absorbance at 550 nm was measured using the VersaMax Microplate Reader.

Cell viability was determined from the expression

$$\text{Cell viability}(\%) = \frac{\text{Absorbance of treated cells}}{\text{Absorbance of control}} \times 100$$

To obtain $GI_{50}$ and $LC_{50}$ values, the absorbance readings were plotted against logarithmic concentration on GraphPad Prism Version 5.01. $GI_{50}$ and $LC_{50}$ values were interpolated from the graphs as concentrations corresponding to the following absorbance values:

$$\text{Absorbance at } GI_{50} = \frac{\text{Absorbance at } T_0 + \text{Absorbance of control}}{2}$$

$$\text{Absorbance at } LC_{50} = \frac{\text{Absorbance at } T_0}{2}$$

## Acknowledgments

The authors acknowledge the National University of Singapore (postgraduate scholarship to H.L. Ng, Academic Research Fund Tier 1 grant R-148-000-153-112 to W.K. Chui and R-148-184-112 to E.H. Chew) and National Medical Council (NMRC/NIG/0050/2009 to E.H. Chew) for financial support.

## References

[1] R. Morphy, Z. Rankovic, Designed multiple ligands. An emerging drug discovery paradigm, J. Med. Chem. 48 (2005) 6523–6543.
[2] L.M. Espinoza-Fonseca, The benefits of the multi-target approach in drug design and discovery, Bioorg Med. Chem. 14 (2006) 896–897.
[3] N.M. O'Boyle, M.J. Meegan, Designed multiple ligands for cancer therapy, Curr. Med. Chem. 18 (2011) 4722–4737.
[4] E.M. Berman, L.M. Werbel, The renewed potential for folate antagonists in contemporary cancer chemotherapy, J. Med. Chem. 34 (1991) 479–485.
[5] I.M. Kompis, K. Islam, R.L. Then, DNA and RNA synthesis: antifolates, Chem. Rev. 105 (2005) 593–620.
[6] M. Visentin, R. Zhao, I.D. Goldman, The antifolates, Hematol. Oncol. Clin. North Am. 26 (2012) 629–648 ix.
[7] E.J. Modest, G.E. Foley, M.M. Pechet, S. Farber, A Series of new, biologically significant dihydrotriazines, J. Am. Chem. Soc. 74 (1952) 855–856.
[8] H.K. Lee, T.M. Rana, Microwave-assisted parallel synthesis of a 4,6-diamino-2,2-dimethyl-1,2-dihydro-1-phenyl-s-triazine library, J. Comb. Chem. 6 (2004) 504–508.
[9] X. Ma, R.S. Woon, P.C. Ho, W.K. Chui, Antiproliferative activity against MCF-7 breast cancer cells by diamino-triazaspirodiene antifolates, Chem. Biol. Drug Des. 74 (2009) 322–326.
[10] X. Ma, W.K. Chui, Antifolate and antiproliferative activity of 6,8,10-triazaspiro [4.5]deca-6,8-dienes and 1,3,5-triazaspiro[5.5]undeca-1,3-dienes, Bioorg Med. Chem. 18 (2010) 737–743.
[11] S. Gromer, S. Urig, K. Becker, The thioredoxin system – from science to clinic, Med. Res. Rev. 24 (2004) 40–89.
[12] E.S. Arner, A. Holmgren, Physiological functions of thioredoxin and

thioredoxin reductase, Eur. J. Biochem. 267 (2000) 6102–6109.
[13] K. Kahlos, Y. Soini, M. Saily, P. Koistinen, S. Kakko, P. Paakko, A. Holmgren, V.L. Kinnula, Up-regulation of thioredoxin and thioredoxin reductase in human malignant pleural mesothelioma, Int. J. Cancer 95 (2001) 198–204.
[14] Y. Soini, K. Kahlos, U. Napankangas, R. Kaarteenaho-Wiik, M. Saily, P. Koistinen, P. Paaakko, A. Holmgren, V.L. Kinnula, Widespread expression of thioredoxin and thioredoxin reductase in non-small cell lung carcinoma, Clin. Cancer Res. 7 (2001) 1750–1757.
[15] S.J. Kim, Y. Miyoshi, T. Taguchi, Y. Tamaki, H. Nakamura, J. Yodoi, K. Kato, S. Noguchi, High thioredoxin expression is associated with resistance to docetaxel in primary breast cancer, Clin. Cancer Res. 11 (2005) 8425–8430.
[16] J. Raffel, A.K. Bhattacharyya, A. Gallegos, H. Cui, J.G. Einspahr, D.S. Alberts, G. Powis, Increased expression of thioredoxin-1 in human colorectal cancer is associated with decreased patient survival, J. Lab. Clin. Med. 142 (2003) 46–51.
[17] W. Cai, L. Zhang, Y. Song, B. Wang, B. Zhang, X. Cui, G. Hu, Y. Liu, J. Wu, J. Fang, Small molecule inhibitors of mammalian thioredoxin reductase, Free Radic. Biol. Med. 52 (2012) 257–265.
[18] J. Lu, A. Holmgren, Thioredoxin system in cell death progression, Antioxid. Redox Signal 17 (2012) 1738–1747.
[19] S. Urig, K. Becker, On the potential of thioredoxin reductase inhibitors for cancer therapy, Seminars Cancer Biol. 16 (2006) 452–465.
[20] F.F. Gan, K.K. Kaminska, H. Yang, C.Y. Liew, P.C. Leow, C.L. So, L.N. Tu, A. Roy, C.W. Yap, T.S. Kang, W.K. Chui, E.H. Chew, Identification of Michael acceptor-centric pharmacophores with substituents that yield strong thioredoxin reductase inhibitory character correlated to antiproliferative activity, Antioxid. Redox Signal 19 (2013) 1149–1165.
[21] B. Zhang, D. Duan, C. Ge, J. Yao, Y. Liu, X. Li, J. Fang, Synthesis of xanthohumol analogues and discovery of potent thioredoxin reductase inhibitor as potential anticancer agent, J. Med. Chem. 58 (2015) 1795–1805.
[22] C.I. Bliss, The toxicity of poisons applied jointly, Ann. Appl. Biol. 26 (1939) 585–615.
[23] S. Loewe, The problem of synergism and antagonism of combined drugs, Arzneimittelforschung 3 (1953) 285–290.
[24] T.C. Chou, P. Talalay, Quantitative analysis of dose-effect relationships: the combined effects of multiple drugs or enzyme inhibitors, Adv. Enzyme Regul. 22 (1984) 27–55.
[25] Y. Grabovsky, R.J. Tallarida, Isobolographic analysis for combinations of a full and partial agonist: curved isoboles, J. Pharmacol. Exp. Ther. 310 (2004) 981–986.
[26] N. Geary, Understanding synergy, Am. J. Physiol. Endocrinol. Metab. 304 (2013) E237–E253.
[27] V. Cody, J.R. Luft, W. Pangborn, Understanding the role of Leu22 variants in methotrexate resistance: comparison of wild-type and Leu22Arg variant mouse and human dihydrofolate reductase ternary crystal complexes with methotrexate and NADPH, Acta Crystallogr. D. Biol. Crystallogr. 61 (2005) 147–155.
[28] A.N. Jain, Surflex: fully automatic flexible molecular docking using a molecular similarity-based search engine, J. Med. Chem. 46 (2003) 499–511.
[29] R. Spitzer, A.N. Jain, Surflex-Dock: docking benchmarks and real-world application, J. Comput. Aided Mol. Des. 26 (2012) 687–699.